Conference paper
Griffo, Antonio, Wang, J.B. and Howe, D. (2008) *State-space average modelling of 18-pulse diode rectifier.* In: 3rd International Conference "From Scientific Computing to Computational Engineering". 3rd IC-SCCE, 9 - 12 July 2008, Athens, Greece.

STATE-SPACE AVERAGE MODELLING OF 18-PULSE DIODE RECTIFIER

Antonio Griffo[1], Jiabin Wang[1] , David Howe[1]

[1] Department of Electronic and Electrical Engineering
University of Sheffield
Mappin Street, S1 3JD Sheffield, UK
e-mail: a.griffo@sheffield.ac.uk, j.b.wang@sheffield.ac.uk

Keywords: Power electronics, AC-DC conversion, State-space averaging

Abstract. *The paper presents an averaged-value model of the direct symmetric topology of 18-pulse autotransformer AC-DC rectifiers. The model captures the key features of the dynamic characteristics of the rectifiers, while being time invariant and computationally efficient. The developed models, validated by comparison of the resultant transient and steady state behaviours with those obtained from detailed simulations can, therefore, be used for stability assessment of electric power systems with diode rectifiers, multiple power electronic converter-controlled loads and electrical drives[*].*

1 INTRODUCTION

The technological trend towards an increased utilisation of electrical power in "more electric" vehicles is posing new challenges in terms of modelling and analysis. Complex power systems, such as those currently investigated for future aircrafts applications, result from the interconnection of several nonlinear and time-varying components with dynamics whose time-scales span several orders of magnitude, ranging from relatively slow phenomena related to generator's voltage or mechanical loads regulations to comparatively faster electrical transients caused by the high frequency switching of power electronics based devices. Due to their switching behaviour power electronics based converters, widely used for dc supplies and for inverter-fed electrical drives, are intrinsically variable structure systems with the algebraic-differential equations describing their dynamics changing in correspondence with the switching events. Averaging techniques have been proposed to filter out high frequency switching behaviour of power electronics devices[1]-[2], allowing computationally efficient analysis of relatively slower dynamics such as those involved in the destabilizing phenomena which may arise due to the interaction between tightly regulated loads and energy storage components[3]-[4].

Averaged value models of 6-pulse and 12-pulse AC to DC converters have been derived in the past[5]-[7] also taking into account the complex interactions with a synchronous generator[8]-[9]. However more complex arrangements such as 18-pulse rectifiers are required for future "more electric" aircrafts in order to comply with stringent requirements on the quality of power supply to both AC and DC loads for military and civilian aircrafts[10]-[11]. Several different topologies of 18-pulse rectifiers have been proposed each with particular advantages and drawbacks[12][13].

After a circuital description of the model employed, the averaged-value model of the direct symmetric topology of 18-pulse AC-DC rectifier is analytically derived in the paper. The model is shown to capture the key features of the dynamic characteristics of the rectifier while being time invariant and computationally efficient. Comparisons of the resultant transient and steady state behaviours with those obtained from detailed simulations are presented to validate the analytically derived equations. The obtained model can therefore be used for stability assessment of electric power systems with diode rectifiers, multiple power electronic converter-controlled loads and electrical drives.

2 STATE SPACE AVERAGING

State-space averaging is extensively used for analysis and control design of switching power electronics converters[1]-[2]. For periodic waveforms *x(t)* the fundamental component state-space averaging is given by the one-cycle average:

$$\langle x \rangle(t) = \frac{1}{T} \int_{t-T}^{t} x(\tau) d\tau \qquad (1)$$

where T is the period. Differentiating (1) with respect to time the following key property of the state-space average is obtained:

$$\frac{d}{dt}\langle x \rangle(t) = \left\langle \frac{d}{dt} x(t) \right\rangle \qquad (2)$$

Equations (1) and (2) are the DC component of the generalized multi-frequency averaging technique[2]. Alternative averaging methods have been proposed to consider systems of differential equations with discontinuous right-hand side[1].

3 AVERAGE MODELLING OF 18-PULSE RECTIFIER

A schematic of the direct symmetric topology for the 18-pulse rectifier is shown in Fig. 1. Three sets of three phase voltages constituting a nine-phase voltage system are generated by an Auto-Transformer (AT) from the three-phase input voltages. Several winding arrangements have been proposed to generate the required phase-shift of ±40 electrical degrees[12][13]. Three three-phase diode bridge rectifiers are connected to the nine-phase source, whereas their DC output terminals are directly connected in parallel. Each diode conducts the DC current for 1/18th of a fundamental period. DC and AC currents transformed to a synchronous reference are therefore periodic with $T=1/(18*f)$, where f is the generator's fundamental frequency. An equivalent schematic of the Auto-Transformer Rectifier Unit (ATRU) is illustrated in Fig. 2, where Lac is the equivalent AT leakage and cable inductance reflected to the secondary. An RLC passive filter is connected at the output of the rectifier.
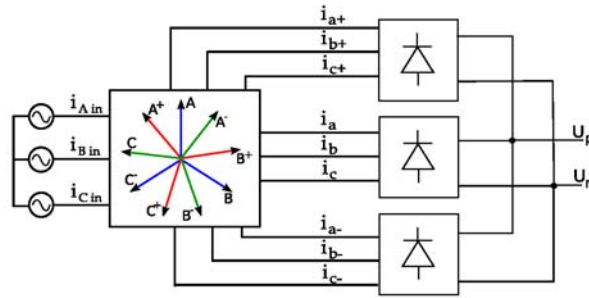
Figure 1: Schematic of a 18-pulse autotransformer and rectifier unit connected to an AC source
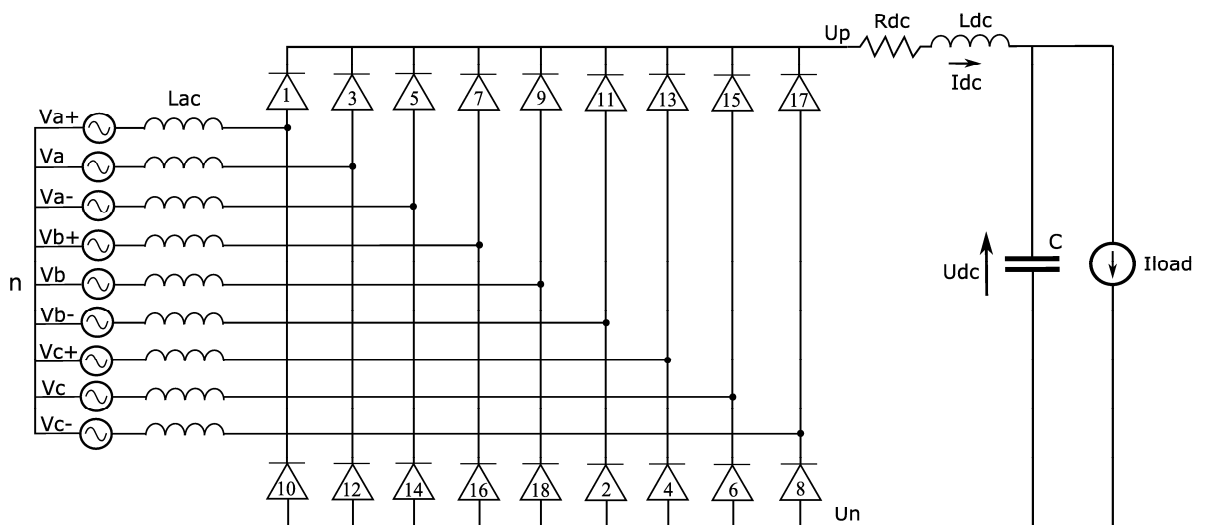
Figure 2: Schematic of the equivalent circuit of the 18-pulse rectifier
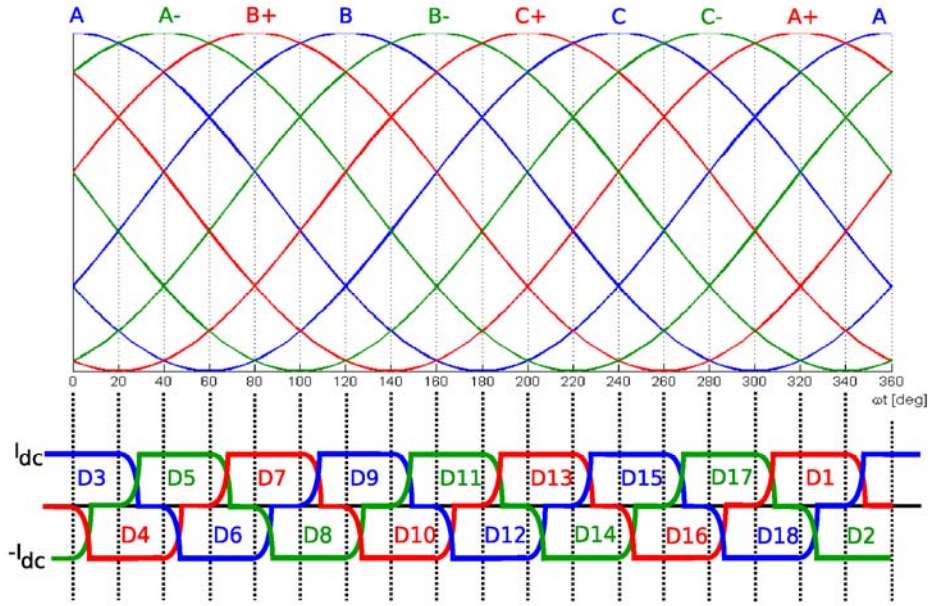
Figure 3: Nine-phase voltages and diode conduction sequence

The ideal nine-phase voltage system generated by the AT is shown in Fig. 3 along with rectifier's diode conduction sequence. The DC current i_{dc} during conduction is assumed constant in the following derivations. The commutation angle μ can be derived by analyzing the commutation process with appropriate boundary conditions as:

$$\mu = \arccos\left(1 - \frac{\omega L_{ac} i_{dc}}{V_m \sin \pi/9}\right) \tag{3}$$

where $\omega = 2\pi f$ and V_m is the AC voltage magnitude.

3.1 DC current with commutation angle μ less than $\pi/9$ rad

Figures 4 and 5 show the ATRU equivalent circuit and the diodes currents during the commutation process from phase B- to C+. The 20 electrical degree interval is divided into two periods: commutation and conduction.
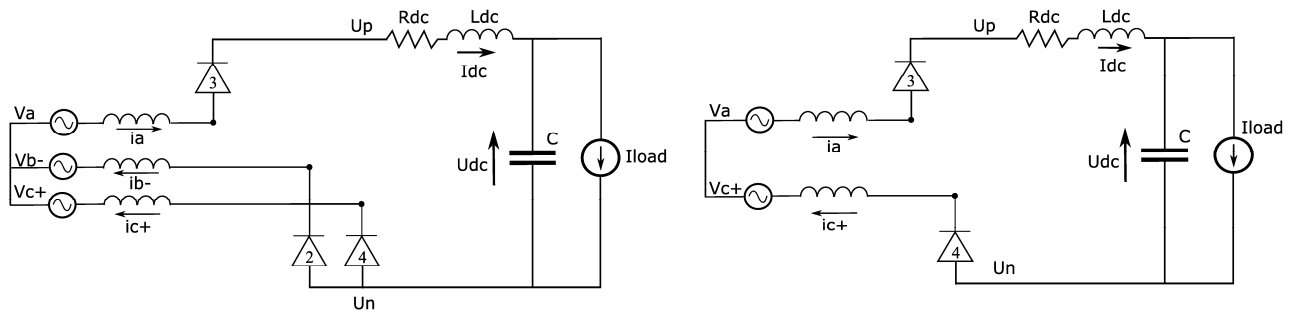
Figure 4: ATRU equivalent circuit during commutation (left) and conduction (right)
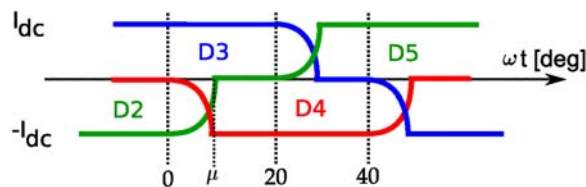
Figure 5: Commutation process with μ less than $\pi/9$ rad

The equations governing phase currents during commutation, i.e. for $0 \leq \omega t \leq \mu$ when D2, D3 and D4 conduct contemporaneously, are given by:

$$L_{ac}\frac{di_a}{dt} = -R_{ac}i_a + V_a - U_p \tag{4a}$$

$$L_{ac}\frac{di_{b-}}{dt} = -R_{ac}i_{b-} + V_{b-} - U_n \tag{4b}$$

$$L_{ac}\frac{di_{c+}}{dt} = -R_{ac}i_{c+} + V_{c+} - U_n \tag{4c}$$

while the DC current is governed by:

$$L_{dc}\frac{di_{dc}}{dt} = -R_{dc}i_{dc} + U_p - U_n - U_{dc} \tag{5}$$

Combining (4a)-(4c) and (5) with the current equations obtained by integrating (4b)-(4c):

$$i_a = i_{dc}$$

$$i_{b-} = -i_{dc} + \frac{V_m}{\omega L_{ac}}\sin\frac{\pi}{9}(1 - \cos\omega t) \tag{6}$$

$$i_{c+} = -\frac{V_m}{\omega L_{ac}}\sin\frac{\pi}{9}(1 - \cos\omega t)$$

and the voltages relationships:

$$V_a = V_m\cos\omega t$$

$$V_{b-} = -V_m\cos(\omega t + \pi/9) \tag{7}$$

$$V_{c+} = -V_m\cos(\omega t - \pi/9)$$

yields:

$$\left(\frac{3}{2}L_{ac} + L_{dc}\right)\frac{di_{dc}}{dt} = -\left(\frac{3}{2}R_{ac} + R_{dc}\right)i_{dc} + V_m[1 + \cos(\pi/9)]\cos\omega t - U_{dc} \tag{8}$$

The equations governing phase currents during conduction, i.e. for $\mu \leq \omega t \leq \pi/9$ when D3 and D4 conduct, are given by:

$$L_{ac}\frac{di_a}{dt} = -R_{ac}i_a + V_a - U_p$$

$$L_{ac}\frac{di_{c+}}{dt} = -R_{ac}i_{c+} + V_{c+} - U_n \tag{9}$$

with:

$$i_a = i_{dc}$$

$$i_{c+} = -i_{dc} \tag{10}$$

The DC link current equation is given by:

$$(2L_{ac} + L_{dc})\frac{di_{dc}}{dt} = -(2R_{ac} + R_{dc})i_{dc} + V_m\cos\omega t + V_m\cos(\omega t - \pi/9) - U_{dc} \tag{11}$$

Taking state-space average (1) over the π/9 period of the DC current eqs. (8) and (11) and using (2) results in

$$\frac{di_{dc}}{dt} = -\left[\frac{9}{\pi}\left(\frac{R_{D1}}{L_{D1}} - \frac{R_{D2}}{L_{D2}}\right)\mu + \frac{R_{D2}}{L_{D2}}\right]i_{dc}$$

$$+ \frac{9}{\pi}V_m\left\{\left[\frac{1}{L_{D1}}(1 + \cos\pi/9) - \frac{1}{L_{D2}}\right]\sin\mu + \frac{1}{L_{D2}}[\sin\pi/9 - \sin(\mu - \pi/9)]\right\} \tag{12}$$

$$- \frac{9}{\pi}U_{dc}\left(\frac{1}{L_{D1}} - \frac{1}{L_{D2}}\right)\mu - \frac{1}{L_{D2}}U_{dc}$$

where:

$$L_{D1} = 3/2 L_{ac} + L_{dc} \qquad L_{D2} = 2L_{ac} + L_{dc}$$
$$R_{D1} = 3/2 R_{ac} + R_{dc} \qquad R_{D2} = 2R_{ac} + R_{dc}$$

(13)

3.2 DC current with commutation angle μ greater than π/9 rad

Figures 6 and 7 show the ATRU equivalent circuit and the diodes currents during the commutation process from phase B- to C+ when the commutation angle is greater than *π/9* rad. The 20 electrical degree interval is divided into two periods: commutations from D1 to D3 and from D2 to D4, and commutation from D2 to D4 while D3 is conducting.
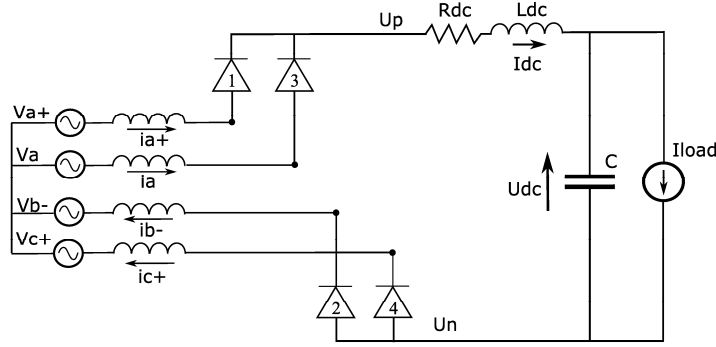
Figure 6: ATRU equivalent circuit during commutation for $0 \le \omega t \le \mu - \pi/9$
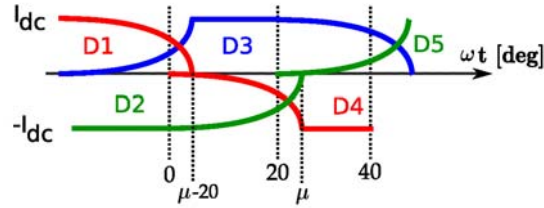
Figure 7: Commutation process with μ greater than $\pi/9$

The equations governing phase currents for $0 \le \omega t \le \mu - \pi/9$ when D1, D2, D3 and D4 conduct are given by:

$$L_{ac} \frac{di_{a+}}{dt} = -R_{ac}i_{a+} + V_{a+} - U_p$$
$$L_{ac} \frac{di_a}{dt} = -R_{ac}i_a + V_a - U_p$$
$$L_{ac} \frac{di_{b-}}{dt} = -R_{ac}i_{b-} + V_{b-} - U_n$$
$$L_{ac} \frac{di_{c+}}{dt} = -R_{ac}i_{c+} + V_{c+} - U_n$$

(14)

which can be integrated giving:

$$i_{a+} = i_{dc} - \frac{V_m}{\omega L_{ac}} \sin \frac{\pi}{9} \left[1 - \cos\left(\omega t + \frac{\pi}{9}\right)\right]$$
$$i_a = \frac{V_m}{\omega L_{ac}} \sin \frac{\pi}{9} \left[1 - \cos\left(\omega t + \frac{\pi}{9}\right)\right]$$
$$i_{b-} = -i_{dc} + \frac{V_m}{\omega L_{ac}} \sin \frac{\pi}{9} \left[1 - \cos\left(\omega t + \frac{\pi}{9}\right)\right]$$
$$i_{c+} = -\frac{V_m}{\omega L_{ac}} \sin \frac{\pi}{9} \left[1 - \cos\left(\omega t + \frac{\pi}{9}\right)\right]$$

(15)

Combining the DC current equation (5) with (15) yields:

$$\frac{di_{dc}}{dt} = -\frac{R_{D3}}{L_{D3}}i_{dc} + \frac{V_m}{L_{D3}}\cos\frac{\pi}{9}\left[\cos\left(\omega t + \frac{\pi}{9}\right) + \cos\omega t\right] - \frac{1}{L_{D3}}U_{dc} \tag{16}$$

where:

$$L_{D3} = L_{ac} + L_{dc} \qquad R_{D3} = R_{ac} + R_{dc} \tag{17}$$

Analogously, the equation governing the DC current for $\mu - \pi/9 \le \omega t \le \pi/9$ when the commutation from D1 to D3 has been terminated with D2, D3 and D4 being conducting is given by:

$$\frac{di_{dc}}{dt} = -\frac{R_{D1}}{L_{D1}}i_{dc} + \frac{V_m}{L_{D1}}\left(1 + \cos\frac{\pi}{9}\right)\cos\omega t - \frac{1}{L_{D1}}U_{dc} \tag{18}$$

Applying state-space averaging to equations (16) and (18), it results:

$$\begin{aligned}
\frac{di_{dc}}{dt} = & -\frac{9}{\pi}\left[\frac{R_{D3}}{L_{D3}}\left(\mu - \frac{9}{\pi}\right) + \frac{R_{D1}}{L_{D1}}\left(\frac{2\pi}{9} - \mu\right)\right]i_{dc} \\
& + \frac{9}{\pi}V_m\left\{\frac{1}{L_{D3}}\cos\frac{\pi}{9}\left[\sin\mu - \sin\frac{\pi}{9} + \sin\left(\mu - \frac{\pi}{9}\right)\right] + \frac{1 + \cos\pi/9}{L_{D1}}\left[\sin\frac{\pi}{9} - \sin\left(\mu - \frac{\pi}{9}\right)\right]\right\} \\
& - \frac{9}{\pi}\left[\frac{1}{L_{D3}}\left(\mu - \frac{\pi}{9}\right) + \frac{1}{L_{D1}}\left(\frac{2\pi}{9} - \mu\right)\right]U_{dc}
\end{aligned} \tag{19}$$

3.3 AC currents

Analytical expression of the three phase AC input currents to the autotransformer unit $i_{Ain}, i_{Bin}, i_{Cin}$ can be obtained from the analysis of the winding arrangment of Fig. 8:

$$\begin{aligned}
i_{Ain} &= i_3 - i_2 + i_a + i_{a-} + i_{a+} \\
i_{Bin} &= i_2 - i_1 + i_b + i_{b-} + i_{b+} \\
i_{Cin} &= i_1 - i_3 + i_c + i_{c-} + i_{c+}
\end{aligned} \tag{20}$$

Transformer magneto-motive force (mmf) balance equations are derived as:

$$\begin{aligned}
i_1 &= 1/N_1(i_{a+} - i_{a-}) + 1/N_2(i_{b-} - i_{c+}) \\
i_2 &= 1/N_1(i_{c+} - i_{c-}) + 1/N_2(i_{a-} - i_{b+}) \\
i_3 &= 1/N_1(i_{b+} - i_{b-}) + 1/N_2(i_{c-} - i_{a+})
\end{aligned} \tag{21}$$

where the transformer winding turn ratios necessary to generate the ±40deg phase shifts are given by $N_1=3.41$, $N_2=6.41$[13]. The averaging procedure has similarly been applied to the AC currents (20), although the results are not reported here due to space limitation.
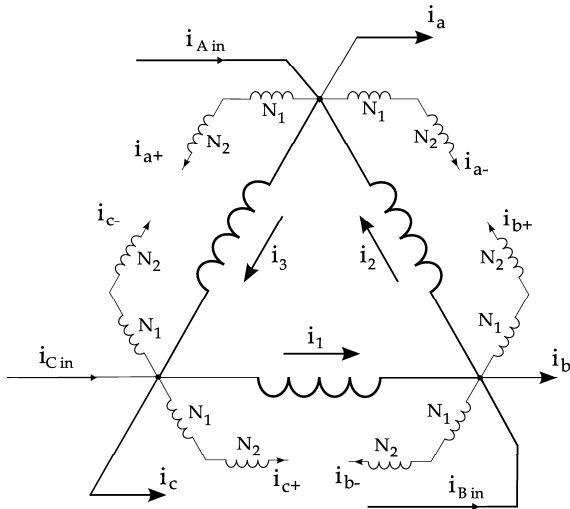
Figure 8: Autotransformer winding arrangement
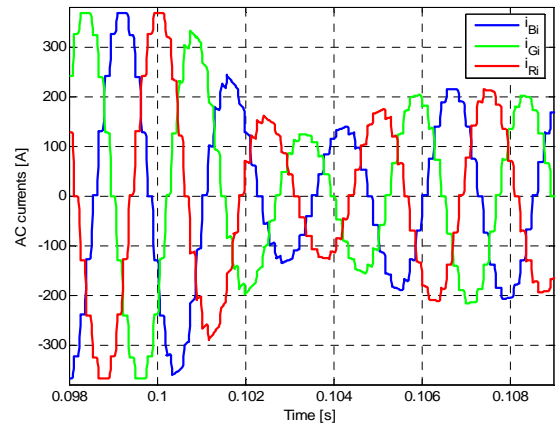
Figure 9: AC current waveforms of ATRU when supplying a resistive load

4 NUMERICAL SIMULATIONS

Numerical simulations have been carried out to validate the analytically derived model by comparing the resulting waveforms with those obtained from simulating a detailed diode-switching model of the ATRU. Figure 9 shows the AC current drawn by the ATRU when it supplies a resistive load whose power consumption is changed from 170kW to 90kW at t=0.1s, while Figs. 10 and 11 compare the steady-state DC voltage and current waveforms obtained from the averaged value model with those of the detailed model after the power variation transient has settled down. Further comparisons are given in Figs. 12 and 13 for the waveforms of d- and q- axis components of the ATRU AC input currents transformed to a synchronously rotating reference frame. As will be seen, a good agreement between the two models in both transient and steady states has been achieved, albeit the switching harmonics due to diode commutations are not present in the averaged value model.
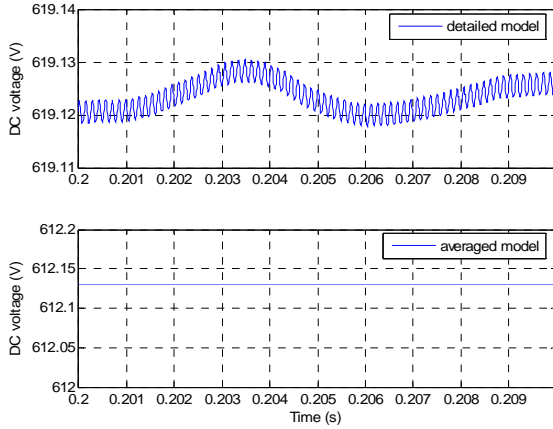
Figure 10: DC voltage obtained with detailed (top) and averaged model (bottom)
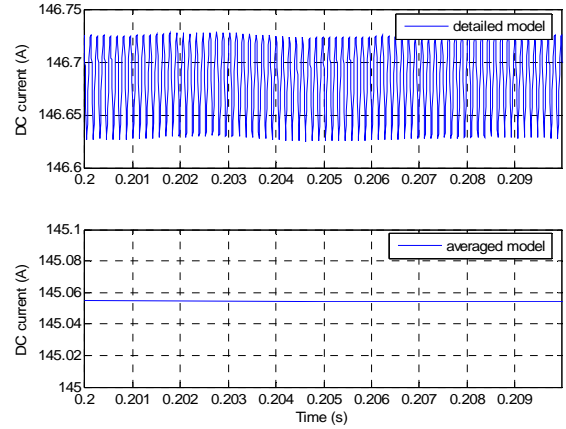
Figure 11: DC current obtained with detailed (top) and averaged model (bottom)
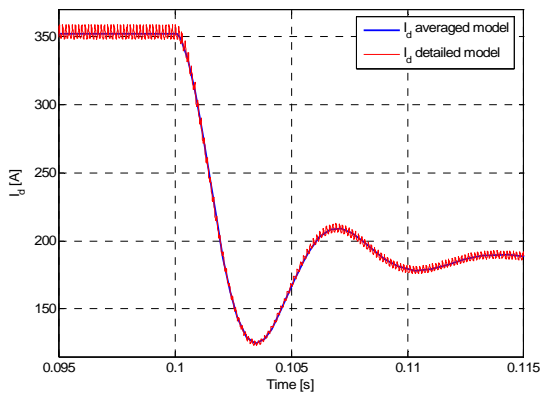
Figure 12: D-axis component of AC currents obtained with detailed (red) and averaged model (blue)
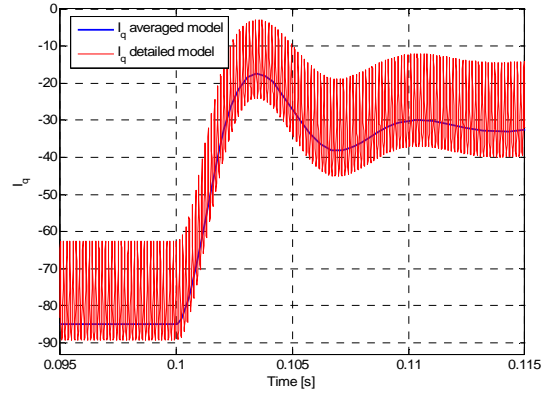
Figure 13: Q-axis component of AC currents obtained with detailed (red) and averaged model (blue)

5 CONCLUSION

An averaged value model for the direct symmetric topology of 18-pulse autotransformer rectifiers has been derived. Comparisons of the transient and steady state behaviors of the model with those obtained from simulations of the detailed diode-switching model have shown that the analytically derived model can capture the key dynamic characteristics of the ARTU. The model can be used for computationally efficient stability assessment of complex electric power systems which employ the 18-pulse ATRU for AC-DC power conversion, such as those currently considered for future "more electric" aircraft.

ACKNOWLEDGEMENT

REFERENCES

[1] Krein, P.T., Bentsman, J., Bass, R.M., Lesieutre, B.L., "On the use of averaging for the analysis of power electronic systems", IEEE Trans. Power Electronics, vol. 5, n. 2, Apr. 1990, pp. 182-190

[2] Sanders, S.R., Noworolski J.M., Liu X.Z., Verghese G.C., "Generalized averagin method for power conversion circuits", IEEE Trans. Power Electronics, vol. 6, n. 2, Apr. 1991, pp. 251-259

[3] Emadi, A.; Khaligh, A.; Rivetta, C.H.; Williamson, G.A., "Constant power loads and negative impedance instability in automotive systems: definition, modeling, stability, and control of power electronic converters and motor drives", IEEE Trans. on Vehicular Technology, vol. 55, n. 4, July 2006 pp. 1112-1125

[4] Han L., Wang J., Howe D., "Stability assessment of distributed DC power systems for 'more electric' aircraft", *Proc. 4ᵗʰ IET International conference on Power Electronics, Machines and Drives*, York, UK, 2008, pp. 661-665.

[5] Zhu, H., Burgos, R.P., Lacaux, F., Uan-Zo-li, A., Lindner, D.K., Wang, F., Boroyevich, D., 2005, "Average modeling of three-phase and nine-phase diode rectifiers with improved AC current and DC voltage dynamics", 31st Annual Conference of IEEE Industrial Electronics Society, IECON 2005.

[6] Baghramian, A., Forsyth, A.J., "Averaged-value models of twelve-pulse rectifiers for aerospace applications", Second International Conference on Power Electronics, Machines and Drives, 2004. (PEMD 2004).

[7] L. Han, J. Wang and D. Howe, "State space average modelling of 6- and 12-pulse diode rectifiers", Proc. of 12ᵗʰ European Conference on Power Electronics and Applications (EPE) 2007, Aalborg, Denmark, Paper ID 639. 2007.

[8] Sudhoff, S.D., Wasynczuk, O., "Analysis and average-value modeling of line-commutated converter-synchronous machine systems", IEEE Trans. on Energy Conversion, vol. 8, n. 1, Mar. 1993, pp. 92-99.

[9] Jatskevich, J., Pekarek, S.D., Davoudi, A., "Fast procedure for constructing an accurate dynamic average-value model of synchronous machine-rectifier systems", IEEE Trans. on Energy Conversion, vol. 21, n.2, June 2006, 435-441

[10] Singh, B.; Gairola, S.; Singh, B.N.; Chandra, A.; Al-Haddad, K., "Multipulse AC–DC Converters for Improving Power Quality: A Review", IEEE Trans. on Power Electronics, vol. 23, n. 1, Jan. 2008 pp. 260-281

[11] USA Department of Defense, "MIL-STD 704F Aircraft electric power characteristics", March 2004

[12] Uan-Zo-li, A., Burgos, R., Wang, F., Boroyevich, D., Lacaux, F., Tardy, A., "Comparison of prospective topologies for aircraft autotransformer-rectifier units", The 29th Annual Conference of the IEEE Industrial Electronics Society, IECON '03.

[13] Chivite-Zabalza, F.J., Forsyth, A.J., Trainer, D.R., "Analysis and practical evaluation of an 18-pulse rectifier for aerospace applications", Second International Conference on Power Electronics, Machines and Drives, 2004.

[14] Mohan, N., Undeland, T., Robbins, W., "Power electronics: converters applications and design", 3ʳᵈ edition, New York, Wiley, 2002